

We E106 10

## Reflection FWI for both Reflectivity and Background Velocity

G. Yao\* (Imperial College London), M. Warner (Imperial College London) & A. Silverton (Imperial College London)

### SUMMARY

---

The application of full-waveform inversion to pure reflection data in the absence of a highly accurate starting velocity model is difficult. We demonstrate a means of achieving this successfully by interleaving least-squares RTM with a version of FWI in which the tomographic gradient that is required to update the background macro-model is separated from the reflectivity gradient using the Born approximation during forward modelling. This provides a good update to the macro-model. This approach is then followed by conventional reflection FWI to obtain a final high-fidelity high-resolution result from a poor starting model using only reflection data.

## Introduction

Three-dimensional full-waveform inversion (FWI) has been successfully applied to field datasets to update the velocity macro model, which can in turn dramatically improve PSDM results. However, conventional FWI on field data used in this way must meet some tough conditions: firstly, long-offset data are normally required with turning energy reaching to the velocity target; secondly, the initial model must be close to the true model; and thirdly, low frequencies, typically reaching down to around 3 to 4 Hz are required in the field data. These conditions apply because conventional FWI works to update the macro model at long wavelengths principally by using transmitted arrivals, and these then are especially vulnerable to the detrimental effects of cycle skipping. In practice, conventional FWI has been most-productively applied in this way to OBC and similar surveys that are dominated by refracted waves. Conventional FWI does not so easily update the macro model when it is applied to reflection-dominated datasets, for example moderate-offset towed-streamer surveys targeting deeper reservoirs.

There are two main reasons why reflection FWI is difficult. Firstly, the initial model must be extremely accurate in order to migrate reflectors correctly into depth, at which point reflection FWI comes gradually to resemble PSDM plus post-stack inversion albeit in a formulation that properly honours the wave equation. Secondly, the gradient generated by conventional FWI typically favours updating reflector amplitudes more than it favours updating the background macro-velocity model.

To solve this problem, and to push FWI to work better with pure reflection data, we here explore alternating inversion schemes that include two steps. The first step is to build temporary reflectors, which will be rebuilt after the second step. The second step is then to update the background velocity model using the reflections generated by the temporary reflectors. By alternating these steps, the background velocity model can be successively improved, and the reflections become more focused. A key additional ingredient is to formulate the methodology so that it does not require an unduly accurate starting model, and to modify the raw gradient so that it favours macro-velocity updates.

## Theory

Standard FWI is implemented by minimising the objective function of the  $L_2$ -norm of the data residual which is the difference between the predicted and observed data. This minimisation is generally achieved with an iterative inversion algorithm that updates the model guided by the direction of the local gradient of the objective function. If such a scheme is applied to pure reflection data with a smooth initial velocity model, then standard FWI progresses as illustrated in Figure 1.

In the first iteration, modelling of the source wavefield does not generate reflections. The forward wavefield therefore consists only of transmitted arrivals, and the residual wavefield consists of only the back-propagated observed data. Relative to the amplitudes in the forward wavefield, the back-propagated wavefield will have amplitudes that are of the order of the reflectivity  $R$ . The cross-correlation of these wavefields will build a reflector into the model which will also have reflectivity of order  $R$ . Although FWI is being used, the dominant effect will be to perform a version of reverse-time migration (RTM) on the observed data using the starting model as the migration velocity field.

During the second iteration, the forward wavefield will consist of a transmitted wavefield with a similar amplitude to that in the first iteration, plus a reflected wavefield of amplitude  $R$ . The back-propagated wavefield will contain its own transmitted wavefield which will be of order  $R$ , plus a reflection of this wavefield which will be of order  $R^2$ . Cross-correlating the forward and backward wavefields will then continue to build the reflector with an update that is proportional to  $R$ , and will begin to update the macro model everywhere above the reflector with an update that is proportional to  $R^2$ . The former effect is reflectivity migration; the latter effect is velocity tomography. Now, since  $|R| \ll 1$ , the update of the reflectivity will be much stronger than the update of the background velocity. Continued iteration will continue to attempt to match the observed data by adjusting the reflectivity, and will minimally improve the match by adjusting the macro model.

From this heuristic analysis, it can be seen that there are two key issues that need to be solved in this system. One of these is to build reflectors in their correct locations in the absence of the correct macro-model, and the other is to find an effective means to update the macro model usefully when the fundamental algorithm being used focuses the majority of its effort upon short-wavelength reflectivity and not upon longer-wavelength background velocity. To solve the latter problem, we must enhance the tomographic aspects of FWI with respect to its migration aspects, and to solve the former problem, we must rebuild the reflectivity as the macro-model evolves and improves.

To do this, we here use an alternating inversion scheme. In the first step, we use either a least-squares reverse-time migration (LS-RTM) or conventional FWI to build reflectors. In the second step, we use a wavefield or gradient decomposition method during FWI to generate the gradient of the macro-model without updating the reflectivity. Having updated the macro-model, we then re-migrate in the first step, and iterate this two-stage process.

The necessary gradient decomposition can be achieved in several ways which include: (a) separating the scattered and incident wavefields using the Born approximation during the forward modelling; (b) separating up-going and down-going wavefields; (c) using a local Poynting-vector for wavefield separation; (d) muting the incident wavefield on migrated angle-gathers; or (e) using scale separation of the gradient by filtering in the wave-number domain. In general, none of these methods can produce perfect separation in complicated models, but they can enhance tomography with respect to migration. In this study, we demonstrate this alternating scheme using methods (a) and (e), and we combine these in various combinations with LS-RTM and conventional FWI.

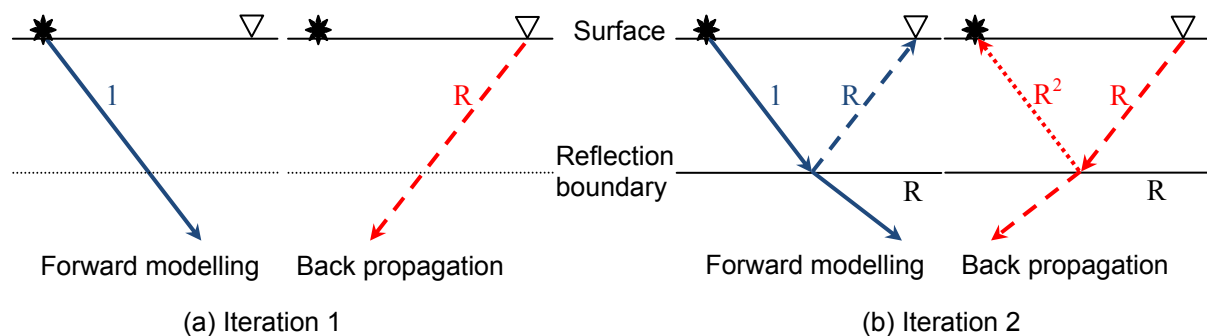


**Figure 1** Behaviour of standard FWI for pure reflection data using a smooth starting model. (a) At the first iteration, only transmitted energy exists in both the forward and back-propagated wavefields. Cross-correlating these builds reflectivity and does not update velocity. (b) At subsequent iterations, reflected energy exists in both wavefields. Cross-correlation can now update the velocity model, but the magnitude of this tomographic effect varies as  $R^2$ , whereas updates to the reflectivity vary as  $R$ .

### Application to a synthetic example

The Marmousi model is easy to invert using long-offsets, turning energy, low frequencies, and an accurate starting model. Here we attempt to invert this model using only short offsets, muting the data to remove refracted energy, using a 10 Hz source wavelet, and an inaccurate starting model, Figures 2 and 3. This is a much more challenging proposition, and it much more closely represents the reality of most field datasets than does the approach typically used to invert Marmousi.

Figure 2 shows synthetic data generated using the Marmousi model. Figure 2(a) shows the full wavefield at the surface receivers; Figure 2(b) shows the data that we invert in which all early-arrival refracted energy has been muted. The maximum offset that we include in the inversion is 3500 m

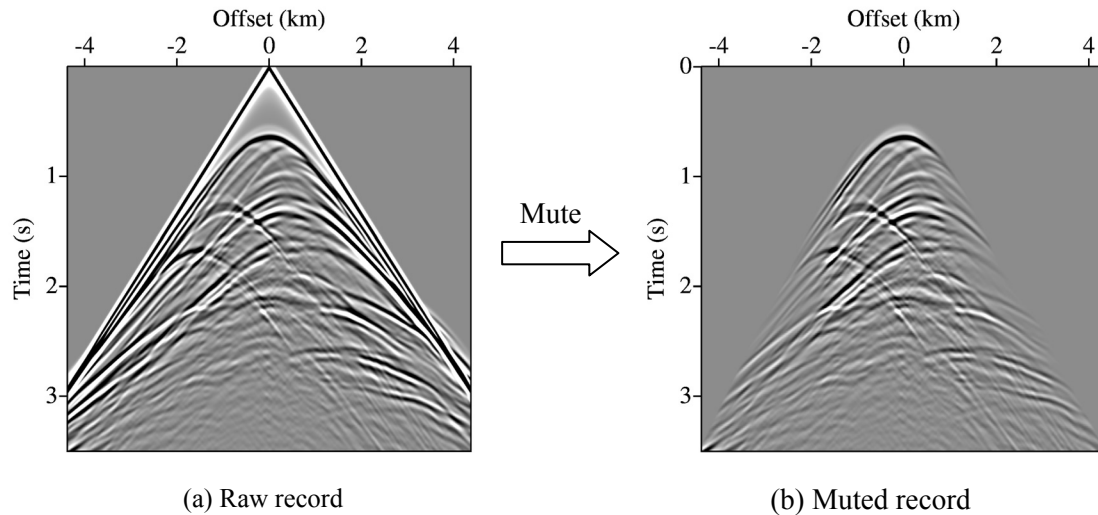


**Figure 2** Synthetic data from Marmousi. The data that we invert are first muted to remove refracted arrivals, and we limit the maximum offset to 3500 m.

which is of a similar size to the depth to the target. We used about 500 sources, a 10 Hz Ricker wavelet, and source and receiver spacing of 25 m and 12.5 m respectively. Figure 3 shows (a) the true model, (b) the one-dimensional inaccurate starting model, and (c) to (f) the results of various inversion schemes.

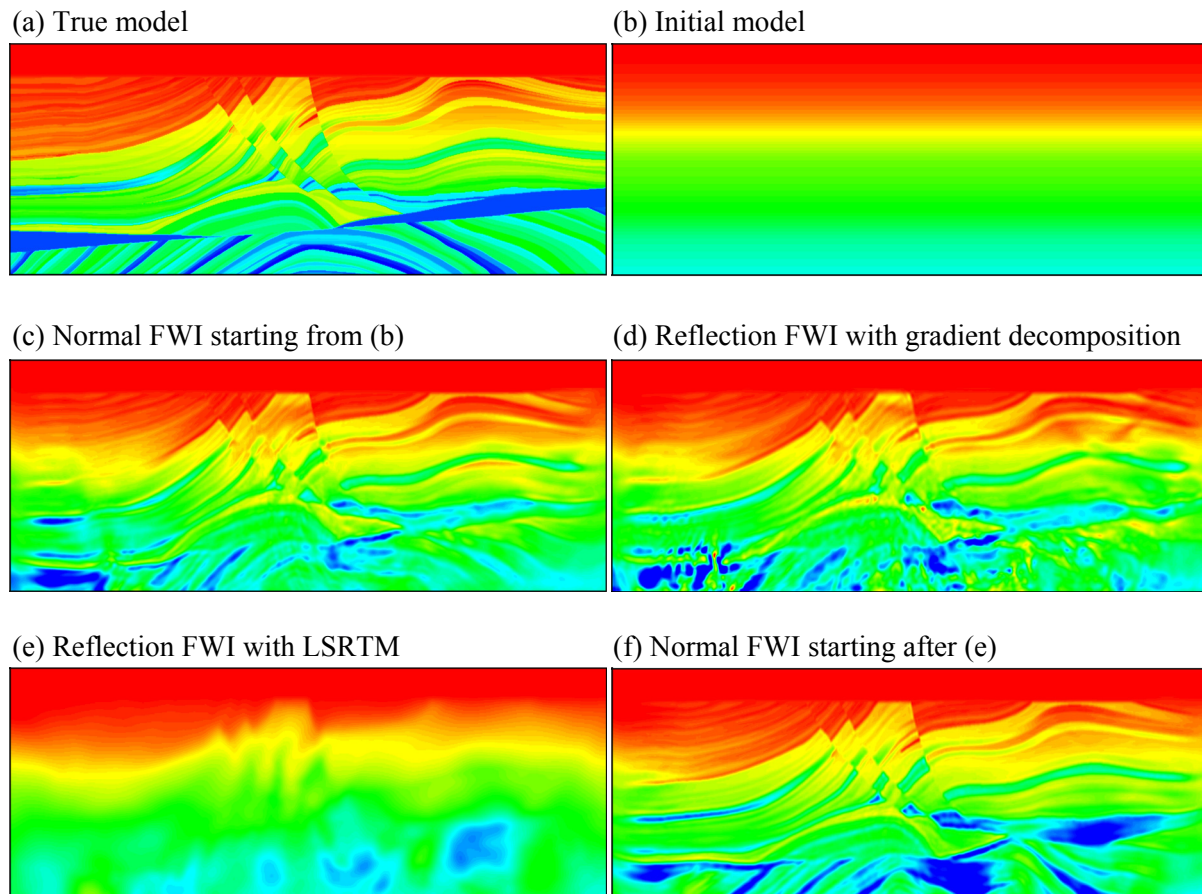
Figure 3(c) shows the results of conventional FWI applied to these data using this starting model, beginning at low frequencies in these noise-free data, and working successively towards higher frequencies. The results of this are reasonably accurate for the top half of the model, but degrade with increasing depth. In part, the high quality of this simple result is an indication that the Marmousi model is, despite its apparent complexity, remarkably easy to invert provided that sufficiently low frequencies are available. Closer examination also shows that this conventional result is not quantitatively correct, even in the shallowest portions of the model, where the initial and true model differed significantly. The model obtained is not sufficiently accurate, for example, for full-bandwidth RTM.

Figure 3(d) shows the results of FWI in which the gradient has been filtered to separate reflectivity and macro-velocity updates by assuming that the former have shorter wavelengths than the latter. The inversion operates using several successive iterations to update the reflectivity; only the shortest-offset data are used for this step. This is then followed by several iterations to update the macro-model using all the data to a maximum offset of 3500 m. The two models are stored separately, but added together to drive the forward modelling. The process is then iterated, rebuilding the reflectivity model again from scratch using the new macro model. The separation of the gradient using scale length is imperfect, and these imperfections influence the quality of the final inversion. In parts of the model, the quantitative match using this method is an improvement on conventional FWI, but in other places, the match deteriorates.

Figure 3(e) shows the results of using least-squares RTM to build the reflectivity, and using the Born approximation to separate the wavefields. In this implementation, the reflectivity and macro-model are stored and update separately. The forward and backward wavefields are each modelled twice – once using only the macro model to generate the transmitted wavefield, and once by applying the Born approximation to these wavefields to generate the primary reflected wavefield. This approach does not correctly deal with multiple reflections. Iterating this as a two-step process, and throwing away the reflectivity at each iteration, generates a smooth update to the macro model. The resultant model is an improvement on the starting model, but it does not of course capture the shortest

wavelengths that cause the reflectivity. The resultant model though is sufficiently accurate for depth migration, at least at the lower end of the reflection bandwidth.

Figure 3(f), which is our preferred approach, builds upon the model generated in Figure 3(e). This shows the results of applying conventional reflection FWI using the model first generated for Figure 3(f). Since this model is adequate for depth migration, conventional FWI is expected to work well for pure reflection data. Figure 3(f) demonstrates this – the model provides a significantly better quantitative match to the true model than does conventional FWI alone, or than does any gradient decomposition method alone. We stress that this result has been reached without refracted arrivals, and with only short-offset reflections in which the maximum offset is similar to the target depth.



**Figure 3** (a) True velocity model; (b) Inaccurate starting model; (c) Conventional FWI; (d) FWI with gradient decomposition by scale length; (e) Macro model combining LS-RTM wavefield decomposition via the Born approximation; (f) Conventional FWI following method (e).

## Conclusions

The alternating scheme and its two implementations, namely reflection FWI with LS-RTM and reflection FWI with gradient decomposition, can be used for velocity recovery from reflection-dominated datasets. Neither of these alone provides a complete solution if the starting model is inadequate. However, the first of these can be used successfully to precondition the starting model such that conventional reflection FWI can then proceed towards an accurate final model. This approach appears to provide a robust and general solution to reflection FWI.